An erbium(III)-based NIR emitter with a highly conjugated *β*-diketonate for blue-region sensitization

P. Martín-Ramos[a,b*], I. R. Martín[b], F. Lahoz[b], S. Hernández-Navarro[a], P. S. Pereira da Silva[c], I. Hernández-Campo[d,e], V. Lavín[c] and M. Ramos Silva[c]

[a] Advanced Materials Laboratory, ETSIIAA, Universidad de Valladolid, Avenida de Madrid 44, 34004 Palencia, Spain. Tel: +34 979 108347; E-mail: pablomartinramos@gmail.com

[b] Department of Physics and MALTA Consolider Team, Universidad de La Laguna, E-38206 San Cristóbal de La Laguna, Santa Cruz de Tenerife, Spain.

[c] CEMDRX, Physics Department, Universidade de Coimbra, Rua Larga, P-3004-516, Coimbra, Portugal.

[d] CITIMAC Dept., Facultad de Ciencias, University of Cantabria, Avenida Los Castros s/n, 39005 Santander, Spain.

[e] School of Physics and Astronomy, Queen Mary University of London, Mile End Road, London E1 4NS, UK

Abstract

The sensitization of lanthanide complexes in the visible region is of particular interest for practical applications such as labeling, biological analysis and optoelectronics. A visible-light sensitized Er^{3+} complex based on the use of a highly conjugated *β*-diketonate (1,3-di(2-naphthyl)-1,3-propanedione, Hdnm) and 5-nitro-1,10-phenanthroline ($5NO_2phen$) as an ancillary ligand, [$Er(dnm)_3(5NO_2phen)$], has been synthesized, fully characterized and its photophysical properties have been investigated. Suitably expanded π-conjugation in the complex molecule makes the excitation window red-shifted to the visible region (up to 550 nm). Efficient energy transfer by antenna effect results in 1.53 μm emission from the Er^{3+} ion.

Keywords: erbium(III), *β*-diketonate, antenna effect, near-infrared, photoluminescence

1. Introduction

Fostered by potential applications in medical imaging and optical telecommunications, there is an increasing interest in the design of lanthanide complexes that exhibit near-infrared (NIR) luminescence [1]. NIR emission has been reported to have advantages for biological applications in terms of medical imaging resolution, detection sensitivity and transmittance of the tissues, as noted by Sun *et al*. [2]. In addition, NIR-emitters can also find applications in active and passive optical architectures [3-7], solar energy conversion [8-10] and sensory technology [11,12].

Nevertheless, 4*f*–4*f* electronic transitions of lanthanide (Ln^{3+}) ions are forbidden by parity and spin rules, leading to very small absorption cross-sections and low molar absorptivities. This drawback can be circumvented by resourcing to suitable strong absorbers, which can sensitize the lanthanide ion *via* the so-called *antenna effect* [13]. This two-step excitation process has been successfully exploited using various organic based sensitizers [14] and transition metal fragments covalently linked to lanthanide complexes [15-18].

The efficiency of the sensitization process is largely dependent on the energy level scheme of the ligands, which should be such that it maximizes the energy transfer path. Thus, the triplet state of the sensitizer must be closely matched to, or slightly above, the lanthanide ion's emitting resonance levels, but not so close that thermal back energy transfer competes effectively with Ln^{3+} emission [19,20]. If this requirement is fulfilled, upon excitation of the organic ligand in the UV-VIS range, a large excited-state population can be achieved by using

light fluences four to five orders of magnitude lower than those required for bare ions [21,22]. Most popular ligands are UV-excitable [23], which can be unwanted and even harmful for living tissue, in the case of bio-sensing applications. Furthermore, no cheap pump sources are available in the UV [24]. Thus, one of the growing challenges in the chemistry of the lanthanide ions is to develop NIR luminescent lanthanide complexes that can be sensitized in the visible range (>400 nm).

A promising means of achieving this longer-wavelength ligand-mediated sensitization is through the modification of the ligand molecule with a suitable expanded π-conjugated system, which have a smaller energy gap between the lowest singlet excited state S_1 and the T_1 state. In the early 2000s, in relation to Eu^{3+}-complexes host:guest systems for organic light-emitting diodes (OLEDs), Heeger's group directed their efforts towards the selection of ligands which would allow efficient Föster energy transfer from conjugated polymer hosts to the Eu^{3+}-complexes dopants [25]. This required sufficient spectral overlap between the emission spectrum of the polymer and the absorption spectra of the Eu^{3+} complexes [26,27]. By assessing various highly conjugated *β*-diketonates, they concluded that 1,3-di(2-naphthyl)-1,3-propanedione (Hdnm) ligand had the best spectral overlap with the blue-emitting CN-PPP, leading to fast and efficient energy transfer from the host to the guest and eliminating almost all of the polymer emission. Similar results were obtained by Reynolds *et al*. [28] for polymers such as PPP-OR11 blended with $[Yb(dnm)_3(phen)]$ complexes. More recently, Divya *et al*. [29] have theoretically and empirically confirmed these claims, showing that naphthyl or biphenyl groups in the *β*-diketonate ligands remarkably extend the excitation window of Eu^{3+} complexes towards the visible region (up to 500 nm), resulting in quantum yields above 40%.

Consideration of the foregoing results motivated us to design a new Er^{3+} complex using the 1,3-di(2-naphthyl)-1,3-propanedione or dinaphthoylmethane (Hdnm) ligand, whose absorption band can extend into the visible region, as the main sensitizer, and 5-nitro-1,10-phenanthroline diimide as an ancillary ligand to complete the coordination sphere. The structure of this newly synthesized Er^{3+} complex has been elucidated by single crystal X-ray diffraction, and its thermal stability and photophysical properties have been evaluated. Photoluminescence measurements show that the dnm ligand successfully extends the excitation bands of the Er^{3+} complex to the blue-light region, leading to NIR-emission by antenna effect. Future efforts will focus on OLED devices fabrication using this and other visible-sensitized materials currently under development.

2. Experimental

2.1. *Materials, synthesis and analytical data*

All reagents and solvents employed were commercially available and used as supplied without further purification. All the procedures for complex preparation were carried out under nitrogen and using dry reagents to avoid the presence of water and oxygen, which can quench metal photoluminescence.

Tris(1,3-di(2-naphthyl)-1,3-propanedionate)mono(5-nitro-1,10-phenanthroline)erbium(III), $[Er(dnm)_3(5NO_2phen)]$, was synthesized as follows: under stirring, a 1,3-di(2-naphthyl)-1,3-propanedione (3 mmol) methanol solution (20 ml) was added to 1 mmol of $Er(NO_3)_3{\cdot}5H_2O$ in methanol. The mixture was neutralized by adding potassium methoxide (3 mmol) dropwise under vigorous stirring until potassium nitrate precipitated. KNO_3 was removed by decanting, and 5-nitro-1,10-phenanthroline (1 mmol) was finally added. The mixture was heated to 75 ºC and stirred overnight, then washed with dioxane, and finally dried in vacuum to give product in 90-95% yield (based on Er^{3+}). Crystals suitable for X-ray analysis were obtained by slow evaporation of a methanol-dioxane solution at room temperature (RT).

$[Er(dnm)_3(5NO_2phen)]$: Chemical formula: $C_{81}H_{52}ErN_3O_8$, M_W: 1362.55. Anal. Calcd. for $C_{81}H_{52}ErN_3O_8$: C, 71.40; H, 3.85; Er, 12.28; N, 3.08; O, 9.39. Found: C, 71.83; H, 4.05; N, 2.98.

2.2. *X-ray crystallographic analysis*

Prior to structural characterization, a powder diffractogram of the complex was obtained using a Bruker D8 Advance Bragg-Brentano diffractometer, in reflection geometry.

For the determination of the crystal structure by X-ray diffraction, a crystal of the aforementioned compound was glued to a glass fibre and mounted on a Bruker APEX II diffractometer. Diffraction data was collected at room temperature 293(2) K using graphite monochromated MoKα (λ=0.71073 Å). Absorption corrections were made using SADABS [30]. The structure was solved by direct methods using SHELXS-97 [31] and refined anisotropically (non-H atoms) by full-matrix least-squares on F^2 using the SHELXL-97 program [31]. PLATON [32] was used to analyse the structure. Mercury, version 3.3 [33], was used for figure plotting. Atomic coordinates, thermal parameters and bond lengths and angles have been deposited at the Cambridge Crystallographic Data Centre (CCDC). Any request to the CCDC for this material should quote the full literature citation and the reference number CCDC 1006734.

2.3. *Physical and optical measurements*

The C, H, N elemental analyses were conducted using a Perkin Elmer CHN 2400 apparatus.

Differential scanning calorimetry (DSC) data were obtained on a DSC Pyris1 Perkin Elmer instrument, equipped with an intracooler cooling unit at -25 ºC (ethylenglycol-water, 1:1 v/v, cooling mixture), with a heating rate β=10°C/min, under a N_2 purge, 20 mL/min.

Infrared spectra were recorded with a Thermo Nicolet 380 FT-IR apparatus equipped with Smart Orbit Diamond ATR system.

The UV-Vis-NIR diffuse reflectance spectrum of the material in the range from 200 to 2000 nm was measured using an integrating sphere coupled to a spectrophotometer (Agilent Cary 5000) in powder form.

The photoluminescence (PL) spectra in the UV-Vis region and the ligand fluorescence decays were obtained exciting with a 280 nm picosecond pulsed light emitting diode (Edinburgh Instruments EPLED-280), with a typical pulse width of 700 ps, and a 405 nm picosecond pulsed diode laser (Edinburgh Instruments EPL-405), with a typical pulse width of 80 ps, and recorded using a fluorescence spectrometer with a single photon counting multichannel plate photomultiplier and a dedicated acquisition software (Edinburgh Instruments LifeSpec II and F900 software). The NIR PL spectrum was measured exciting the sample using a 450 W Xenon arc lamp followed by a 0.22 m double-grating monochromator (Spex 1680) to provide an excitation beam centred at 450 nm. The NIR emission was focused with a convergent lens onto a 0.18 m single-grating monochromator (Jobin Yvon Triax180, grating 600 grooves/mm) with a resolution of 0.5 nm and then detected with an InGaAs detector. The NIR luminescence decay curves were measured both upon excitation of the ligands at 450 nm and upon direct excitation of Er^{3+} ions at 520 nm with an OPO (Continuum Panther OPO, Laser Photonics) pumped with a Nd-YAG (Surelite) [pulse width: 7 ns; frequency: 10 Hz]. The emitted light was dispersed with a 0.55 m single-grating monochromator (Jobin Yvon Triax550, grating 600 grooves/mm) and detected with a liquid nitrogen-cooled photomultiplier (Hamamatsu R5509-72) and a lock-in amplifier (7265 DSP Perkin Elmer). The lifetime was measured by using a digital oscilloscope (LeCroy 500 MHz). All spectra were corrected for the spectral response of the equipment, and samples were analysed directly as powder.

3. Results and discussion

3.1. *Structural description*

The mononuclear complexes in [Er(dnm)$_3$(5NO$_2$phen)] crystallize in the triclinic space group $P\bar{1}$, with cell parameters a=10.2326(3) Å, b=13.5753(4) Å, c=23.9980(7) Å, α=93.855(2)º, β=96.4920(10)º, γ=110.2500(10)º, V=3087.18(16) Å^3, with two complexes in the unit cell (see Figure 1 and Table 1). In each complex, the Er^{3+} ion is eight-coordinated with six oxygen atoms from the sensitizing ligands (1,3-di(2-naphthyl)-1,3-propanedionate) and two nitrogen atoms from the 5-nitro-1,10-phenanthroline neutral antenna, forming a distorted square-antiprismatic structure. The 5-nitro-1,10-phenanthroline ligand shows some signs of disorder with large thermal ellipsoids in the nitro group. The trivalent erbium ion lies approximately in the middle of the antiprism with a distance of 1.3467(2) Å to the face containing the N atoms and 1.2328(2) Å to the opposite square face containing exclusively O atoms. The angle between the least-squares plane of those square faces is 4.4º. The Er–N distances are 2.564(3) and 2.551(3) Å and the Er–O distances lie in the range 2.247(2)–2.305(2) Å. The N–Er–N bite angle is 63.17(9)º. The complex packs very efficiently in the crystal leaving no solvent accessible voids.

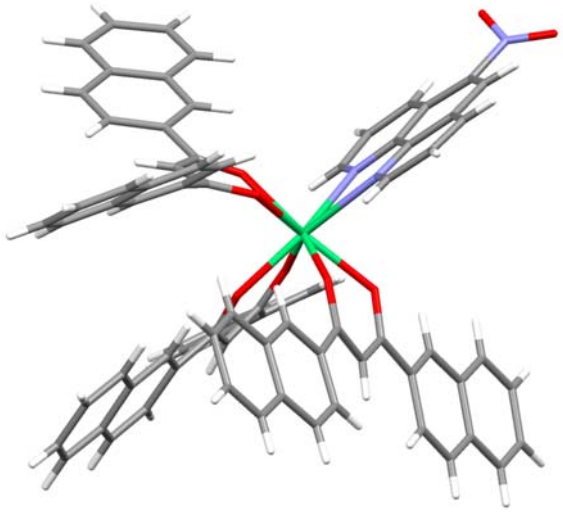

Figure 1. A perspective view of the eightfold coordination of [Er(dnm)$_3$(5NO$_2$phen)].

Table 1. Crystal data and structure refinement for [Er(dnm)$_3$(5NO$_2$phen)] complex

Complex	[Er(dnm)$_3$(5NO$_2$phen)]
Empirical formula	$C_{81}H_{52}ErN_3O_8$
Formula weight	1362.52
Temperature (K)	293(3)
Wavelength (Å)	0.71073
Crystal system	Triclinic
Space group	*P-1*
a (Å)	10.2326(3)
b (Å)	13.5753(4)
c (Å)	23.9980(7)
α (º)	93.855(2)
β (º)	96.4920(10)
γ (º)	110.2500(10)
Volume (Å^3)	3087.18(16)
Z	2
Calculated density (g cm^{-3})	1.466
Absorption coefficient (mm^{-1})	1.424
F(000)	1382

θ range for data collection	3.11-25.72º
Index ranges	-12<*h*<12; -16<*k*<16; -29<*l*<29
Reflections collected	63758
Independent reflections	9873
Completeness to 2θ=51º	99.5%
Refinement method	Full matrix LS on F^2
Data/restrains/parameters	11722/0/838
Goodness-of-fit on F^2	1.179
Final *R* indices [*I*>2σ(*I*)]	*R*=0.0309; w*R*=0.0723
R indices (all data)	*R*=0.0423; w*R*=0.0779
Largest diff. peak and hole	1.088/-0.466

Table 2. Selected distances and angles (Å,º) for [Er(dnm)$_3$(5NO$_2$phen)]

Bond	Distance	Bonds	Angle
Er1-N1	2.564(3)	O1-Er1-O2	71.69(8)
Er1-N2	2.551(3)	O2-Er1-O5	143.51(8)
Er1-O1	2.286(2)	O5-Er1-O6	72.09(8)
Er1-O2	2.303(2)	O6-Er1-O1	144.29(8)
Er1-O3	2.247(2)	O1-Er1-O5	73.05(8)
Er1-O4	2.305(2)	O2-Er1-O6	143.94(8)
Er1-O5	2.300(2)	O3-Er1-O4	72.49(7)
Er1-O6	2.292(2)	O3-Er1-N1	147.09(9)
Er1-N avg.	2.558	O4-Er1-N2	135.67(8)
Er1-O avg.	2.289	N1-Er1-N2	63.17(9)

3.2. *X-ray powder diffraction*

Figure 2 shows the experimental diffraction pattern and the simulated powder diffraction pattern from the single crystal structure using PLATON [32]. There is a good match between simulated and experimental diffractograms: the peaks appear at the predicted theta angles. Differences in intensity can be ascribed to the Bragg-Brentano geometry of the instrument used.

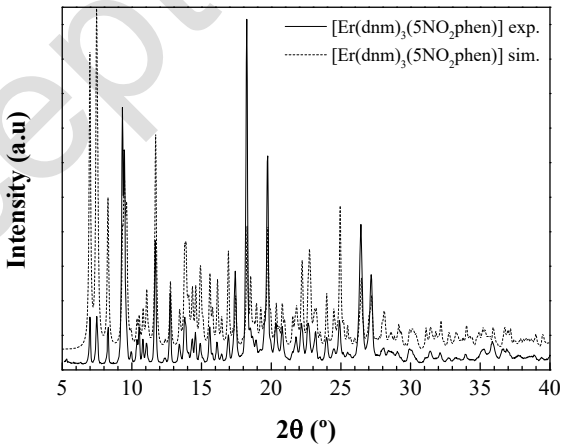

Figure 2. Experimental (*solid line*) *vs*. simulated (*dashed line*) X-ray powder diffraction patterns for [Er(dnm)$_3$(5NO$_2$phen)] complex.

3.3. *Thermal analysis by DSC*

The DSC curve of the complex (under N_2 atmosphere) shows endothermic effects at 152.6 ºC and 228 ºC, and exothermic effects above 240 ºC (see Figure 3). The first endotherm corresponds to melting, while the second one can be associated to partial vaporization/sublimation. When decomposition takes place above 240 ºC, two decomposition exotherms are observed, that can be tentatively attributed to the *β*-diketone ligand (at ca. 252 ºC) and the diimine ligand (at around 276 ºC).

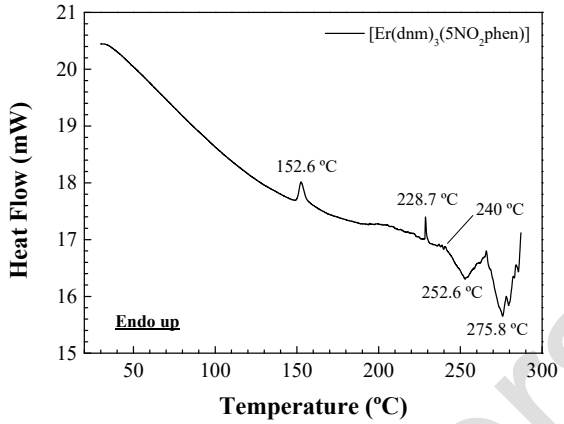

Figure 3. DSC curve of [Er(dnm)$_3$(5NO$_2$phen)] complex.

3.4. *Vibrational characterization*

The IR absorption spectrum for the complex is shown in Figure 4. The absorption bands were identified in accordance with the literature [34-36]: the band at ca. 3050 cm^{-1} must be assigned to =C-H sp^2 aryl vibrations. The bands in the 1340–1627 cm^{-1} region are assigned to symmetric and asymmetric ν(C···N), ν(C···C), ν(C···C···C···O) vibrations. Those in the 733-1016 cm^{-1} range are associated to δ(CH) out-of-plane bending vibrations and γ(CH) in-plane ring breathing modes, both from the naphtyl groups in the *β*-diketonate and from 5-nitro-1,10-phenanthroline. The shifts in their respective frequencies (*vs*. those of free ligands) are due to the perturbations induced by the coordination to the Er^{3+} ion. Finally, vibrations in the region of 400–700 cm^{-1} are to be assigned to ν(Er–O) and ν(Er-N) bonds, in agreement with Tsaryuk *et al.* [36].

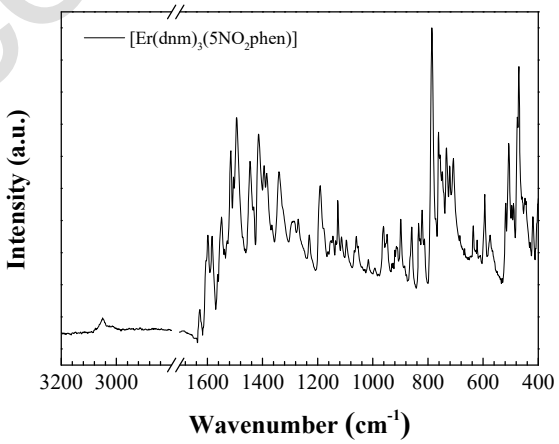

Figure 4. ATR-FTIR spectrum of [Er(dnm)$_3$(5NO$_2$phen)] complex.

3.5. *Absorption spectrum*

The RT diffuse reflectance spectrum of the [Er(dnm)$_3$(5NO$_2$phen)] complex in the UV-visible-NIR range (200-2000 nm) is given in Figure 5. The broad absorption bands in the 200-500 nm range are associated to the π-π* transitions of the dnm (peak at ca. 410 nm) [2] and 5-nitro-1,10-phenanthroline organic ligands (245-320 nm region) [37]. Above 500 nm, sharp peaks associated to intra-configurational $4f^{11}$–$4f^{11}$ electronic transitions starting from the $^4I_{15/2}$ ground state to the different excited levels of the Er^{3+} ion can be observed, superimposed to the ligand absorption. All the absorption bands expected below 500 nm (above 20000 cm^{-1}) are overlapped and masked by the ligand absorption bands. The main bands correspond to the transitions from the $^4I_{13/2}$ ground state to $^2H_{11/2}$ (~522 nm), $^4S_{3/2}$ (~544 nm), $^4F_{9/2}$ (~660 nm), $^4I_{9/2}$ (~802 nm), $^4I_{11/2}$ (~977 nm) and $^4I_{13/2}$ (~1532 nm) Er^{3+} excited states [38]. Figure 5 also shows the second and third overtones of aromatic C–H stretching vibration, which appear near 1675 nm and 1140 nm, respectively.

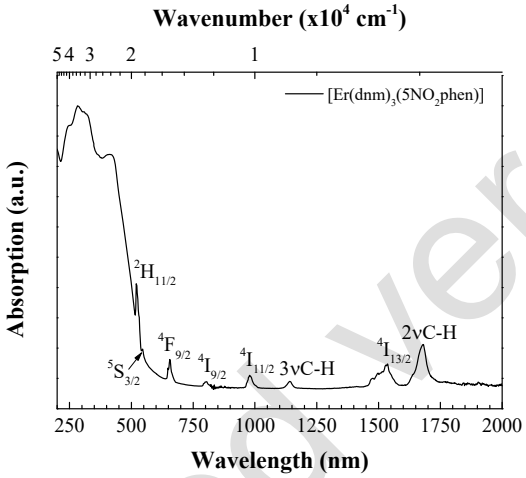

Figure 5. Diffuse reflectance spectrum of the [Er(dnm)$_3$(5NO$_2$phen)] complex in the UV-visible-NIR range at RT. All transitions start from the $^4I_{15/2}$ ground state to the indicated levels.

3.6. *Excitation spectrum and photoluminescence emission*

Photoluminescence in the visible range. The emission from the organic ligands in the UV and visible regions has been studied under direct excitation of the organic ligands at λ_{exc}=280 nm (see Figure 6) and, taking advantage of the broad and red-shifted absorption band of the complex, upon excitation at λ_{exc}=405 nm (see Figure 6). In the former case we can observe some residual emission from the organic part of the complex, with a maximum at around 370 nm. Under 405 nm laser excitation, the emission exhibits another broad band from the ligands burned with Er^{3+}-associated re-absorption bands, arising from the $^2H_{11/2}\rightarrow{}^4I_{15/2}$ transition at around 525 nm and the $^4F_{9/2}\rightarrow{}^4I_{15/2}$ transition at around 650 nm. Since the emission spectra have been measured in powder, it is expected that they may be slightly red-shifted in comparison to those obtained in solution, as a result of the aggregation state.

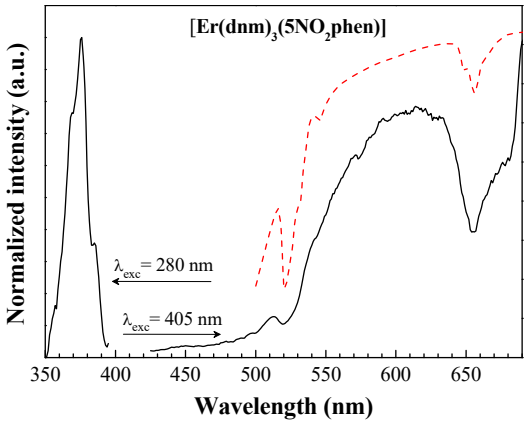

Figure 6. PL emission of [Er(dnm)$_3$(5NO$_2$phen)] complex in the visible region upon excitation at 280 nm and 405 nm. The absorption spectrum (in red) is also included for comparison.

NIR photoluminescence spectrum. The NIR emission spectrum was recorded upon excitation of the organic ligands at 450 nm using a Xe lamp (see Figure 7). A broad emission in the near-IR region is obtained, peaking at around 1530 nm. The emission profile shows some structure associated to the Stark energy levels hyperfine structure and the electron population distributions of the $^4I_{13/2}$ and $^4I_{15/2}$ multiplets.

This emission is the result of an efficient energy transfer from the organic ligands to the Er^{3+} lanthanide ions in the resulting local environment in the complex under study (the so-called *antenna effect*): upon optical excitation in the UV (see Figure 8), the organic ligands are excited from the singlet ground state to a singlet excited state ($S_0 \rightarrow S_n$). The molecule then undergoes *fast internal conversion*, and the S_n state decays into the lowest energy singlet excited state ($S_n \rightarrow S_1$) on the ligand. Ligand singlet excited states S_1 can either decay to the ground state S_0 (*molecular fluorescence*), or to triplet states T_n through an *intersystem crossing* (ISC) mechanism enhanced by heavy atom effect ($S_1 \rightarrow T_1$). The triplet state T_1 can be deactivated radiatively to the S_0 ground state by the spin-forbidden transition $T_1 \rightarrow S_0$, which would result in *molecular phosphorescence*, or the excited triplets can subsequently populate the upper levels of the lanthanide ion via *resonant energy transfer* (RET) [39]. The latter process can occur either via Dexter [40] or Förster [26] mechanisms, depending on total angular momentum variation (ΔJ) undergone by the lanthanide ion [41,42]. After this indirect excitation by energy transfer, the Er^{3+} ion undergoes radiative decay to a lower 4*f* state resulting in the characteristic line-like lanthanide-centered luminescence [12].

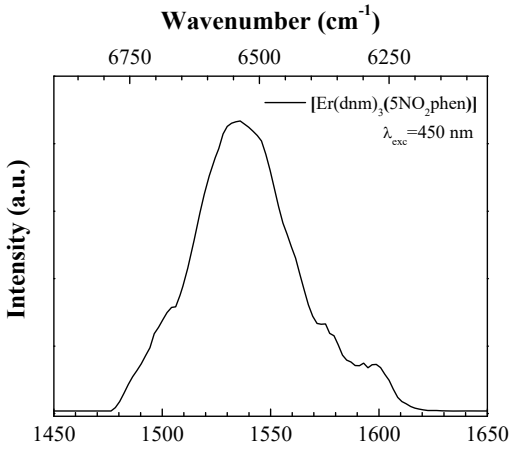

Figure 7. Photoluminescence spectrum in the NIR region upon ligand mediated excitation in the blue region (λ_{exc}=450 nm).

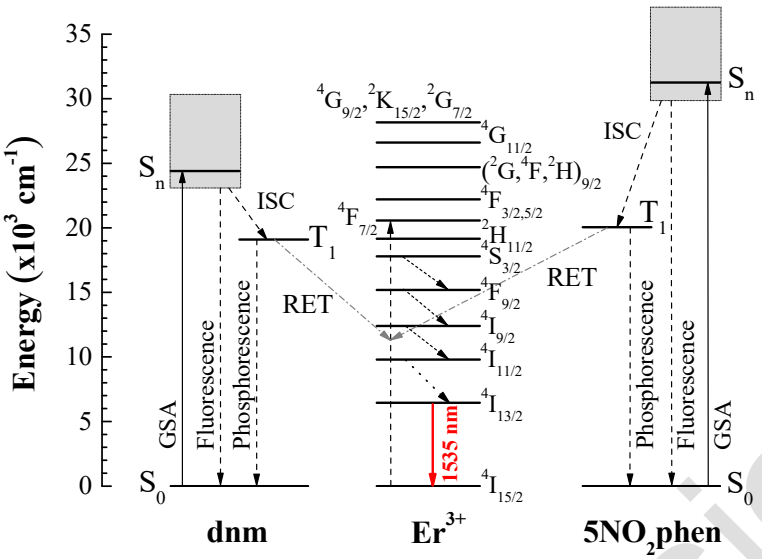

285 **Figure 8**. Scheme of the energy transfer mechanisms and emission processes. The singlet values ($^1\pi\pi^*$=24400 cm^{-1} for dnm and 31250 cm^{-1} for 5NO$_2$phen) have been estimated from the absorption spectrum. The triplet values ($^3\pi\pi^*$=19100 cm^{-1} for dnm and 20048 cm^{-1} for 5NO$_2$phen) have been taken from the literature [2,37]. GSA stands for ground state absorption.

290

Excitation spectrum. The excitation spectrum of the $^4I_{13/2}\rightarrow{}^4I_{15/2}$ emission is shown in Figure 9. It is in good agreement with the excitation spectra reported by Sun *et al.* [2] for analogous complexes. It features a broad band at about 450 nm, which is close to the absorption maximum of the corresponding organic ligands in the UV-Vis absorption spectrum, further 295 confirming that the sensitization of the emissive metal center is by energy transfer mediated by these ligands. The peak at ca. 530 nm can be assigned to the intrinsic Er^{3+} transition $^4I_{15/2}\rightarrow{}^2H_{11/2}$.

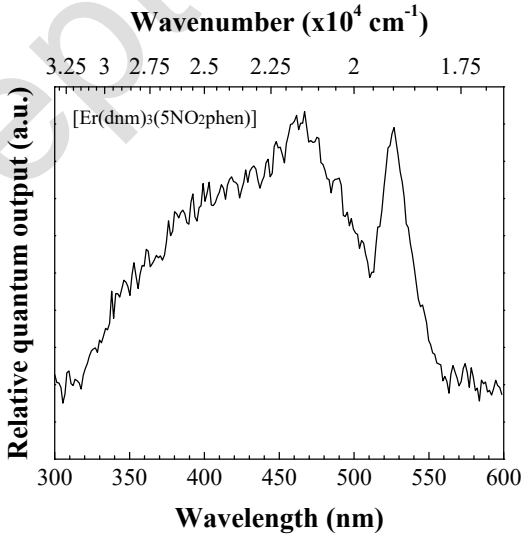

300 **Figure 9.** Excitation spectrum of Er^{3+} in [Er(dnm)$_3$(5NO$_2$phen)] complex monitoring the $^4I_{13/2}\rightarrow{}^4I_{15/2}$ emission at 1530 nm at RT.

3.7. *Lifetime measurements*

305 The decay of the ligand fluorescence was first measured using a high repetition rate pulsed UV diode centered at 280 nm. The detection wavelength was tuned at the maximum of the

$S_1 \rightarrow S_0$ fluorescence band, at 370 nm. The decay of the fluorescence (not shown) was so fast that it could not be resolved with this excitation source. Therefore, this decay was measured again using the significantly faster 405 nm picosecond pulsed diode laser, with a typical pulse width of 80 ps, observing a non-exponential decay (see Figure 10).

The non-exponential character of the decay is characteristic of solid powder samples in which, in addition to the radiative and multiphonon relaxation processes, other interactions - such as ligand-to-ligand and ligand-to-metal interactions contribute to the overall decay of the fluorescence. In order to quantify the average lifetime value of the fluorescence, the decay curve has been successfully fitted to a double exponential decay of the type:

$$I(t) = B_1 \cdot e^{(-t/\tau_1)} + B_2 \cdot e^{(-t/\tau_2)} \quad (1)$$

The fitting was made using IRF reconvolution analysis with F900 software (Edinburgh Instruments). The average lifetime is then calculated using the following equation [43]:

$$\tau_{av} = (B_1\tau_1^2 + B_2\tau_2^2)/(B_1\tau_1 + B_2\tau_2) \quad (2)$$

The obtained average lifetime of the S_1 excited state of [Er(dnm)$_3$(5NO$_2$phen)] complex is about 0.16 ns. This is a relatively short lifetime value, which may be related to an efficient ligand-to-metal energy transfer process.

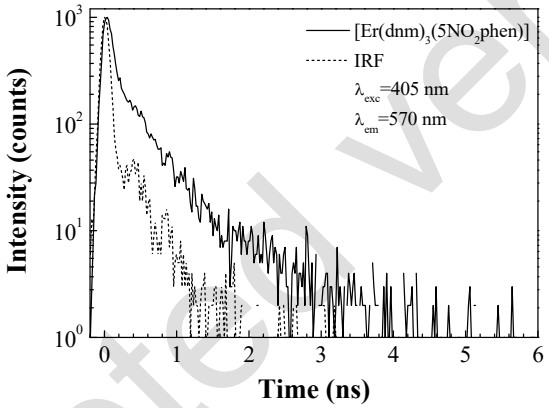

Figure 10. Room temperature PL decay curve of the ligand-associated emission in the visible region upon excitation at 405 nm. The instrument response function is represented as a dashed line.

The NIR PL decay of the $^4I_{13/2}$ multiplet was measured both upon ligand-mediated excitation (at 450 nm) and upon direct excitation of the Er^{3+} ions (at 520 nm) with an OPO laser at 10 Hz repetition rate. The decay shows a single exponential behavior, which can be observed as a linear dependence in the semi-log representations of Figure 11. The good fitting to a single-exponential function confirms a unique and consistent coordination environment around the lanthanide ion [44]. The $^4I_{13/2}$ lifetime value for the complex is τ=1.57 μs, which is similar to other Er^{3+} complexes previously reported by our group (see Table 3) and by other authors (e.g., [45,46]). This value, although almost one order of magnitude larger than that reported for erbium(III) tris(8-hydroxyquinolate) or ErQ_3 (0.2 μs in powder form) [47], is significantly smaller than those attained for Er(F-tpip)$_3$ (where HF-tpip stands for tetrapentafluorophenylimidodiphosphinate) [48] or for perfluorinated nitrosopyrazolone-based erbium chelates [49]: 164 μs and 15.7 μs, respectively. Thus, it can be inferred that perfluorination of *β*-diketonate ligands and the N,N-donor moiety is required so as to further increase the lifetime. If we consider that the radiative lifetime of the $^4I_{13/2}$ excited level ranges around 2–3 ms, the quantum efficiency of the NIR transition of this compound is about 0.1%.

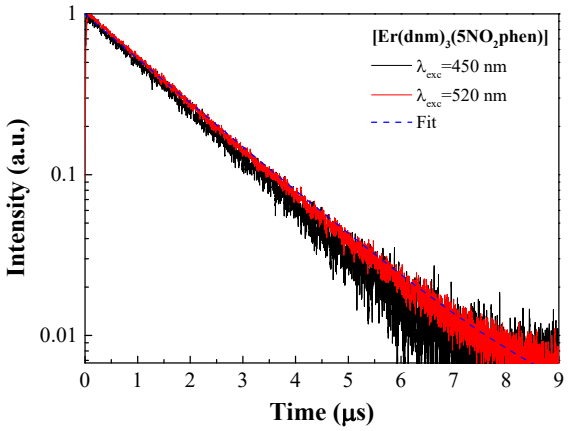

Figure 11. Room temperature PL decay of the $^4I_{13/2}$ multiplet measured under ligand excitation at 450 nm (*black*) and upon direct excitation of Er^{3+} at 520 nm (*red*). The single-exponential fit is also included (*dashed blue line*).

Table 3. PL decay values of the $^4I_{13/2}$ multiplet for several non-fluorinated (*top*) and fluorinated (*bottom*) Er^{3+} *β*-diketonante complexes.

Complexes†	NIR emission lifetime (μs)	Reference
[Er(acac)$_3$(bath)]	1.02	[50]
[Er(dbm)$_3$(bipy)]	1.50	[51]
[Er(h)$_3$(bipy)]	0.97	[52]
[Er(h)$_3$(bath)]	1.16	[52]
[Er(h)$_3$(5NO$_2$phen)]	1.08	[52]
[Er(hd)$_3$(bipy)]	1.05	[53]
[Er(dmh)$_3$(bipy)]	1.67	[54]
[Er(dmh)$_3$(bath)]	1.69	[54]
[Er(dmh)$_3$(5NO$_2$phen)]	1.38	[54]
[Er(thd)$_3$(bath)]	1.38	[55]
[Er(od)$_3$(bipy)]	1.26	[56]
[Er(od)$_3$(bath)]	1.09	[56]
[Er(od)$_3$(5NO$_2$phen)]	1.02	[56]
[Er(nd)$_3$(bipy)]	1.22	[57]
[Er(tfa)$_3$(bipy)]	1.24	[58]
[Er(tfnb)$_3$(bipy)]	1.53	[59]
[Er(tfac)$_3$(bipy)]	1.65	[60]
[Er(tfac)$_3$(bath)]	1.40	[60]
[Er(tfac)$_3$(5NO$_2$phen)]	1.33	[60]
[Er(tpm)$_3$(bipy)]	1.77	[61]
[Er(tpm)$_3$(bath)]	1.55	[61]
[Er(tpm)$_3$(5NO$_2$phen)]	1.53	[61]
[Er(fod)$_3$(bipy)]	1.50	[62]
[Er(fod)$_3$(bath)]	1.39	[62]

† Hacac=acetylacetone, Hdbm= dibenzoylmethane, Hh=2,4-hexanedione, Hhd=3,5-heptanedione, Hdmh=2,6-dimethyl-3,5-heptanedione, Hthd=2,2,6,6,-tetramethyl-3,5-heptanedione, Hod=2,4-octanedione, Hnd=2,4-nonanedione, Htfa=4,4,4-trifluoro-1-(2-furyl)-1,3-butanedione, Htfnb=4,4,4-trifluoro-1-(2-naphthyl)-1,3-butanedione, Htfac=1,1,1-trifluoro-2,4-pentanedione, Htpm=1,1,1-trifluoro-5,5-dimethyl-2,4-hexanedione, Hfod=6,6,7,7,8,8,8-heptafluoro-2,2-dimethyl-3,5-octanedione

4. Conclusions

A new Er^{3+} complex with 1,3-di(2-naphthyl)-1,3-propanedione β-diketonate ligand and 5-nitro-1,10-phenanthroline diimide has been synthesized and its properties studied. The elucidation of the structure of $[Er(dnm)_3(5NO_2phen)]$ by single crystal X-ray diffraction shows that the complex packs very efficiently in the crystal leaving no solvent accessible voids, and thermal analysis confirms good stability up to 240 ºC.

Photoluminescence measurements show that the dnm ligand successfully extends the excitation bands of the Er^{3+} complex to the blue region, allowing sensitization in the visible range and circumventing the problems associated to UV pumping (in terms of cost and for bio-sensing applications). Efficient energy transfer by antenna effect results in 1.53 μm emission from the Er^{3+} ion.

In spite of the fact that the expanded π-conjugation in the complex molecule makes the excitation window red-shifted to the visible region (up to 550 nm) can be regarded as promising, the $^4I_{13/2}$ lifetime (1.57 μs) is still limited by second-sphere matrix interactions and is similar to the majority of Er^{3+} β-diketonate complexes reported to date. Perfluoration of the complex is suggested as a course of action for future work.

Acknowledgments

P. Martín-Ramos would like to thank Iberdrola Foundation for its financial support. Support by MICINN (MAT2010-21270-C04-02, MAT2013-46649-C4-4-P, the Consolider-Ingenio 2010 Program MALTA CSD2007-0045 and the Spanish National Program of Infrastructure), by Caja Canarias Foundation (ENER-01), and by EU-FEDER funds are gratefully acknowledged by La Laguna group. This work was supported by funds from FEDER (Programa Operacional Factores de Competitividade COMPETE) and from FCT-Fundação para a Ciência e a Tecnologia under the Project PEst-C/FIS/UI0036/2014. Access to TAIL-UC facility funded under QREN-Mais Centro Project ICT_2009_02_012_1890 is gratefully acknowledged. P. S. Pereira da Silva also acknowledges FCT for the scholarship SFRH/BPD/84173/2012.

References

[1] S. Faulkner, S.J.A. Pope, B.P. Burton-Pye, Lanthanide Complexes for Luminescence Imaging Applications, ACIAR Proc., 40 (2005) 1-31.

[2] L. Sun, Y. Qiu, T. Liu, H. Peng, W. Deng, Z. Wang, L. Shi, Visible-light sensitized sol–gel-based lanthanide complexes (Sm, Yb, Nd, Er, Pr, Ho, Tm): microstructure, photoluminescence study, and thermostability, RSC Adv., 3 (2013) 26367.

[3] J. Kido, Y. Okamoto, Organo Lanthanide Metal Complexes for Electroluminescent Materials, Chem. Rev., 102 (2002) 2357-2368.

[4] M.A. Katkova, M.N. Bochkarev, New trends in design of electroluminescent rare earth metallo-complexes for OLEDs, Dalton Trans., 39 (2010) 6599.

[5] H.Q. Ye, Z. Li, Y. Peng, C.C. Wang, T.Y. Li, Y.X. Zheng, A. Sapelkin, G. Adamopoulos, I. Hernández, P.B. Wyatt, W.P. Gillin, Organo-erbium systems for optical amplification at telecommunications wavelengths, Nature Mater., 13 (2014) 382-386.

[6] C. Chen, D. Zhang, T. Li, D. Zhang, L. Song, Z. Zhen, Erbium-ytterbium codoped waveguide amplifier fabricated with solution-processable complex, Appl. Phys. Lett., 94 (2009) 041119.

[7] C. Chen, D. Zhang, T. Li, D. Zhang, L. Song, Z. Zhen, Demonstration of Optical Gain at 1550 nm in Erbium–Ytterbium Co-Doped Polymer Waveguide Amplifier, J. Nanosci. Nanotechnol., 10 (2010) 1947-1950.

[8] J.-C.G. Bünzli, S.V. Eliseeva, Lanthanide NIR luminescence for telecommunications, bioanalyses and solar energy conversion, J. Rare. Earth., 28 (2010) 824-842.

[9] Q.Y. Zhang, X.Y. Huang, Recent progress in quantum cutting phosphors, Prog. Mater Sci., 55 (2010) 353-427.

[10] B.M. van der Ende, L. Aarts, A. Meijerink, Lanthanide ions as spectral converters for solar cells, PCCP, 11 (2009) 11081.
[11] J.-C.G. Bünzli, Benefiting from the Unique Properties of Lanthanide Ions, Acc. Chem. Res., 39 (2006) 53-61.
[12] K. Binnemans, Rare-earth beta-diketonates, in: K.A. Gschneidner, J.-C.G. Bünzli, V.K. Pecharsky (Eds.) Handbook on the Physics and Chemistry of Rare Earths, Elsevier B.V., North-Holland, 2005, pp. 107-272.
[13] J.-M. Lehn, Perspectives in Supramolecular Chemistry—From Molecular Recognition towards Molecular Information Processing and Self-Organization, Angew. Chem. Int. Ed., 29 (1990) 1304-1319.
[14] K. Binnemans, Lanthanide-Based Luminescent Hybrid Materials, Chem. Rev., 109 (2009) 4283-4374.
[15] M.R. Sambrook, D. Curiel, E.J. Hayes, P.D. Beer, S.J.A. Pope, S. Faulkner, Sensitised near infrared emission from lanthanides via anion-templated assembly of d-f heteronuclear [2]pseudorotaxanes, New J. Chem., 30 (2006) 1133.
[16] F.-F. Chen, Z.-Q. Bian, Z.-W. Liu, D.-B. Nie, Z.-Q. Chen, C.-H. Huang, Highly Efficient Sensitized Red Emission from Europium (III) in Ir−Eu Bimetallic Complexes by ^{3}MLCT Energy Transfer, Inorg. Chem., 47 (2008) 2507-2513.
[17] R. Ziessel, S. Diring, P. Kadjane, L. Charbonnière, P. Retailleau, C. Philouze, Highly Efficient Blue Photoexcitation of Europium in a Bimetallic Pt–Eu Complex, Chem. Asian J., 2 (2007) 975-982.
[18] N.M. Shavaleev, G. Accorsi, D. Virgili, Z.R. Bell, T. Lazarides, G. Calogero, N. Armaroli, M.D. Ward, Syntheses and Crystal Structures of Dinuclear Complexes Containing d-Block and f-Block Luminophores. Sensitization of NIR Luminescence from Yb(III), Nd(III), and Er(III) Centers by Energy Transfer from Re(I)− and Pt(II)−Bipyrimidine Metal Centers, Inorg. Chem., 44 (2005) 61-72.
[19] R.D. Archer, H. Chen, L.C. Thompson, Synthesis, Characterization, and Luminescence of Europium(III) Schiff Base Complexes, Inorg. Chem., 37 (1998) 2089-2095.
[20] F. Gutierrez, C. Tedeschi, L. Maron, J.-P. Daudey, R. Poteau, J. Azema, P. Tisnès, C. Picard, Quantum chemistry-based interpretations on the lowest triplet state of luminescent lanthanides complexes. Part 1. Relation between the triplet state energy of hydroxamate complexes and their luminescence properties, Dalton Trans., (2004) 1334.
[21] N. Sabbatini, M. Guardigli, J.-M. Lehn, Luminescent lanthanide complexes as photochemical supramolecular devices, Coord. Chem. Rev., 123 (1993) 201-228.
[22] G.F. de Sá, O.L. Malta, C. de Mello Donegá, A.M. Simas, R.L. Longo, P.A. Santa-Cruz, E.F. da Silva, Spectroscopic properties and design of highly luminescent lanthanide coordination complexes, Coord. Chem. Rev., 196 (2000) 165-195.
[23] B. Yan, Recent progress in photofunctional lanthanide hybrid materials, RSC Adv., 2 (2012) 9304.
[24] K. Kuriki, Y. Koike, Y. Okamoto, Plastic Optical Fiber Lasers and Amplifiers Containing Lanthanide Complexes, Chem. Rev., 102 (2002) 2347-2356.
[25] M.D. McGehee, T. Bergstedt, C. Zhang, A.P. Saab, M.B. O'Regan, G.C. Bazan, V.I. Srdanov, A.J. Heeger, Narrow Bandwidth Luminescence from Blends with Energy Transfer from Semiconducting Conjugated Polymers to Europium Complexes, Adv. Mater., 11 (1999) 1349-1354.
[26] T. Förster, 10th Spiers Memorial Lecture. Transfer mechanisms of electronic excitation, Discuss. Faraday Soc., 27 (1959) 7.
[27] A. Dogariu, R. Gupta, A.J. Heeger, H. Wang, Time-resolved Förster energy transfer in polymer blends, Synth. Met., 100 (1999) 95-100.
[28] T.S. Kang, B.S. Harrison, M. Bouguettaya, T.J. Foley, J.M. Boncella, K.S. Schanze, J.R. Reynolds, Near-Infrared Light-Emitting Diodes (LEDs) Based on Poly(phenylene)/Yb-tris(β-Diketonate) Complexes, Adv. Funct. Mater., 13 (2003) 205-210.
[29] V. Divya, R.O. Freire, M.L.P. Reddy, Tuning of the excitation wavelength from UV to visible region in Eu^{3+}-β-diketonate complexes: Comparison of theoretical and experimental photophysical properties, Dalton Trans., 40 (2011) 3257.
[30] G. Sheldrick, SADABS, in, University of Göttingen, Göttingen, Germany, 1996.

[31] G.M. Sheldrick, A short history of SHELX, Acta Crystallogr. Sect. A: Found. Crystallogr., 64 (2007) 112-122.
[32] A.L. Spek, Single-crystal structure validation with the program PLATON, J. Appl. Crystallogr., 36 (2003) 7-13.
[33] C.F. Macrae, P.R. Edgington, P. McCabe, E. Pidcock, G.P. Shields, R. Taylor, M. Towler, J. van de Streek, Mercury: visualization and analysis of crystal structures, J. Appl. Crystallogr., 39 (2006) 453-457.
[34] T.P. Gerasimova, S.A. Katsyuba, Bipyridine and phenanthroline IR-spectral bands as indicators of metal spin state in hexacoordinated complexes of Fe(II), Ni(II) and Co(II), Dalton Trans., 42 (2013) 1787.
[35] K. Nakamoto, Infrared and Raman Spectra of Inorganic and Coordination Compounds, Applications in Coordination, Organometallic, and Bioinorganic Chemistry, 6th ed., Wiley, 2009.
[36] V. Tsaryuk, V. Zolin, J. Legendziewicz, R. Szostak, J. Sokolnicki, Effect of ligand radicals on vibrational IR, Raman and vibronic spectra of europium β-diketonates, Spectrochim. Acta, Pt. A: Mol. Biomol. Spectrosc., 61 (2005) 185-191.
[37] C. Xu, Photophysical properties of lanthanide complexes with 5-nitro-1,10-phenanthroline, Monatsh. Chem., 141 (2010) 631-635.
[38] C. Görller-Walrand, K. Binnemans, Spectral intensities of f-f transitions, in: K.A. Gschneidner, L. Eyring (Eds.) Handbook on the physics and chemistry of rare earths, Elsevier BV, Amsterdam, 1998, pp. 101-264.
[39] B.W. Van Der Meer, G. Coker, S.Y.S. Chen, Resonance Energy Transfer: Theory and Data, Wiley, 1994.
[40] D.L. Dexter, A Theory of Sensitized Luminescence in Solids, J. Chem. Phys., 21 (1953) 836.
[41] M.P. Lowe, D. Parker, pH Switched sensitisation of europium(III) by a dansyl group, Inorg. Chim. Acta, 317 (2001) 163-173.
[42] F. Vögtle, M. Gorka, V. Vicinelli, P. Ceroni, M. Maestri, V. Balzani, A Dendritic Antenna for Near-Infrared Emission of Nd^{3+} Ions, ChemPhysChem, 2 (2001) 769.
[43] J.R. Lakowicz, Principles of fluorescence spectroscopy, 3rd ed., Springer, New York, 2006.
[44] S. Gago, J.A. Fernandes, J.P. Rainho, R.A. Sá Ferreira, M. Pillinger, A.A. Valente, T.M. Santos, L.D. Carlos, P.J.A. Ribeiro-Claro, I.S. Gonçalves, Highly Luminescent Tris(β-diketonate)europium(III) Complexes Immobilized in a Functionalized Mesoporous Silica, Chem. Mater., 17 (2005) 5077-5084.
[45] Z. Li, J. Yu, L. Zhou, H. Zhang, R. Deng, Z. Guo, 1.54 μm Near-infrared photoluminescent and electroluminescent properties of a new Erbium (III) organic complex, Org. Electron., 9 (2008) 487-494.
[46] X. Li, Z. Si, C. Pan, L. Zhou, Z. Li, X. Li, J. Tang, H. Zhang, Near-infrared luminescent properties and natural lifetime calculation of a novel Er^{3+} complex, Inorg. Chem. Commun., 12 (2009) 675-677.
[47] S.W. Magennis, A.J. Ferguson, T. Bryden, T.S. Jones, A. Beeby, I.D.W. Samuel, Time-dependence of erbium(III) tris(8-hydroxyquinolate) near-infrared photoluminescence: implications for organic light-emitting diode efficiency, Synth. Met., 138 (2003) 463-469.
[48] G. Mancino, A.J. Ferguson, A. Beeby, N.J. Long, T.S. Jones, Dramatic Increases in the Lifetime of the Er^{3+} Ion in a Molecular Complex Using a Perfluorinated Imidodiphosphinate Sensitizing Ligand, J. Am. Chem. Soc., 127 (2005) 524-525.
[49] L. Beverina, M. Crippa, M. Sassi, A. Monguzzi, F. Meinardi, R. Tubino, G.A. Pagani, Perfluorinated nitrosopyrazolone-based erbium chelates: a new efficient solution processable NIR emitter, Chem. Commun., (2009) 5103.
[50] P. Martín-Ramos, P.S. Pereira Silva, P. Chamorro-Posada, M. Ramos-Silva, B.F. Milne, F. Nogueira, J. Martín-Gil, Synthesis, structure, theoretical studies and luminescent properties of a ternary erbium(III) complex with acetylacetone and bathophenanthroline ligands, J. Phys. Chem. A, Submitted (2014).
[51] P. Martín-Ramos, J.T. Coutinho, M. Ramos-Silva, L.C.J. Pereira, V. Lavín, F. Lahoz, P. Pereira da Silva, J. Martín-Gil, Single-Ion-Magnet behaviour and photoluminescent properties of a highly coordinated erbium(III) complex with dibenzoylmethane and 2,2'-bipyridine, New J. Chem., Submitted (2014).

[52] M. Ramos Silva, P. Martín-Ramos, J.T. Coutinho, L.C.J. Pereira, J. Martín-Gil, Effect of the capping ligand on luminescent erbium(iii) β-diketonate single-ion magnets, Dalton Trans., 43 (2014) 6752.
[53] P. Martín-Ramos, M.D. Miranda, M.R. Silva, M.E.S. Eusebio, V. Lavín, J. Martín-Gil, A new near-IR luminescent erbium(III) complex with potential application in OLED devices, Polyhedron, 65 (2013) 187-192.
[54] P. Martín-Ramos, V. Lavín, M. Ramos Silva, I.R. Martín, F. Lahoz, P. Chamorro-Posada, J.A. Paixão, J. Martín-Gil, Novel erbium(III) complexes with 2,6-dimethyl-3,5-heptanedione and different N,N-donor ligands for ormosil and PMMA matrices doping, J. Mater. Chem. C, 1 (2013) 5701-5710.
[55] P. Martín-Ramos, M. Ramos Silva, J.T. Coutinho, L.C.J. Pereira, P. Chamorro-Posada, J. Martín-Gil, Single-Ion Magnetism in a Luminescent Er^{3+} β-Diketonato Complex with Multiple Relaxation Mechanisms, Eur. J. Inorg. Chem., 2014 (2014) 511-517.
[56] P.S. Pereira da Silva, P. Martín-Ramos, M. Ramos Silva, V. Lavín, P. Chamorro-Posada, J. Martín-Gil, X-ray analysis, molecular modelling and NIR-luminescence of erbium(III) 2,4-octanedionate complexes with N,N-donors, Polyhedron, 81 (2014) 485-492.
[57] P. Martín-Ramos, P. Chamorro-Posada, M. Ramos Silva, P.S. Pereira da Silva, I.R. Martín, F. Lahoz, V. Lavín, J. Martín-Gil, Synthesis, structural modelling and luminescence of a novel erbium(III) complex with 2,4-nonanedione and 2,2'-bipyridine ligands for chitosan matrices doping, Opt. Mater., Submitted (2014).
[58] M. Ramos Silva, P. Martín-Ramos, J.T. Coutinho, L.C.J. Pereira, V. Lavín, I.R. Martín, P.S. Pereira Silva, J. Martín-Gil, Multiple relaxation mechanisms in Erbium SIMs, Dalton Trans., Submitted (2014).
[59] P. Martín-Ramos, C. Coya, Á.L. Álvarez, M. Ramos Silva, C. Zaldo, J.A. Paixão, P. Chamorro-Posada, J. Martín-Gil, Charge Transport and Sensitized 1.5 μm Electroluminescence Properties of Full Solution-Processed NIR-OLED based on Novel Er(III) Fluorinated β-Diketonate Ternary Complex, J. Phys. Chem. C, 117 (2013) 10020-10030.
[60] P. Martín-Ramos, M.C. Coya-Párraga, V. Lavín, I.R. Martín, M. Ramos Silva, P.S. Pereira Silva, M. García-Vélez, Á.L. Álvarez, J. Martín-Gil, Solution-processed NIR-OLEDs based on ternary erbium(III) complexes with 1,1,1-trifluoro-2,4-pentanedione and different N,N-donors, Dalton Trans., Submitted (2014).
[61] P. Martín-Ramos, M.R. Silva, C. Coya, C. Zaldo, Á.L. Álvarez, S. Álvarez-García, A.M. Matos Beja, J. Martín-Gil, Novel erbium(III) fluorinated β-diketonate complexes with N,N-donors for optoelectronics: from synthesis to solution-processed devices, J. Mater. Chem. C, 1 (2013) 2725-2734.
[62] P. Martín-Ramos, M. Ramos Silva, F. Lahoz, I.R. Martín, P. Chamorro-Posada, M.E.S. Eusebio, V. Lavín, J. Martín-Gil, Highly fluorinated erbium(III) complexes for emission in the C-band, J. Photochem. Photobiol. A: Chem., 292 (2014) 16-25.